Widening Extensive Air Showers Simulations to produce Technological Results

Mauricio Suárez-Durán[1], Christian Sarmiento-Cano[2,3], Antonio Juan Rubio-Montero[4], Álvaro Taboada[2], Raúl Pagán-Muñoz[4], Rolando Calderón-Ardila[2], Luis A. Núñez[3], Iván Sidelnik[5], Rafael Mayo-García[4,*] and Hernán Asorey[2,6]

[1] Université Libre de Bruxelles (ULB), [2] Instituto de Tecnologías en Detección y Astropartículas (ITeDA, CNEA-CONICET-UNSAM), [3] Universidad Industrial de Santander (UIS), [4] Centro de Investigaciones Energéticas, Medioambientales y Tecnológicas (CIEMAT), [5] Departamento de Física de Neutrones (CNEA/CONICET), [6] Departamento Física Médica (CNEA)

[*] rafael.mayo@ciemat.es, presenter

IWARA

From Quarks to Cosmos

IWARA 2022

11th. International Workshop on Astronomy and Relativistic Astrophysics.

Antigua Guatemala, Guatemala.

5 - 9 September, 2022

LAGO

Latin America Giant Observatory

lagoproject.net

EOSC SYNERGY

Horizon 2020 RI project 857647

The Latin American Giant Observatory

LAGO is a giant network of astroparticle detectors at global scale, currently operating in 11 countries

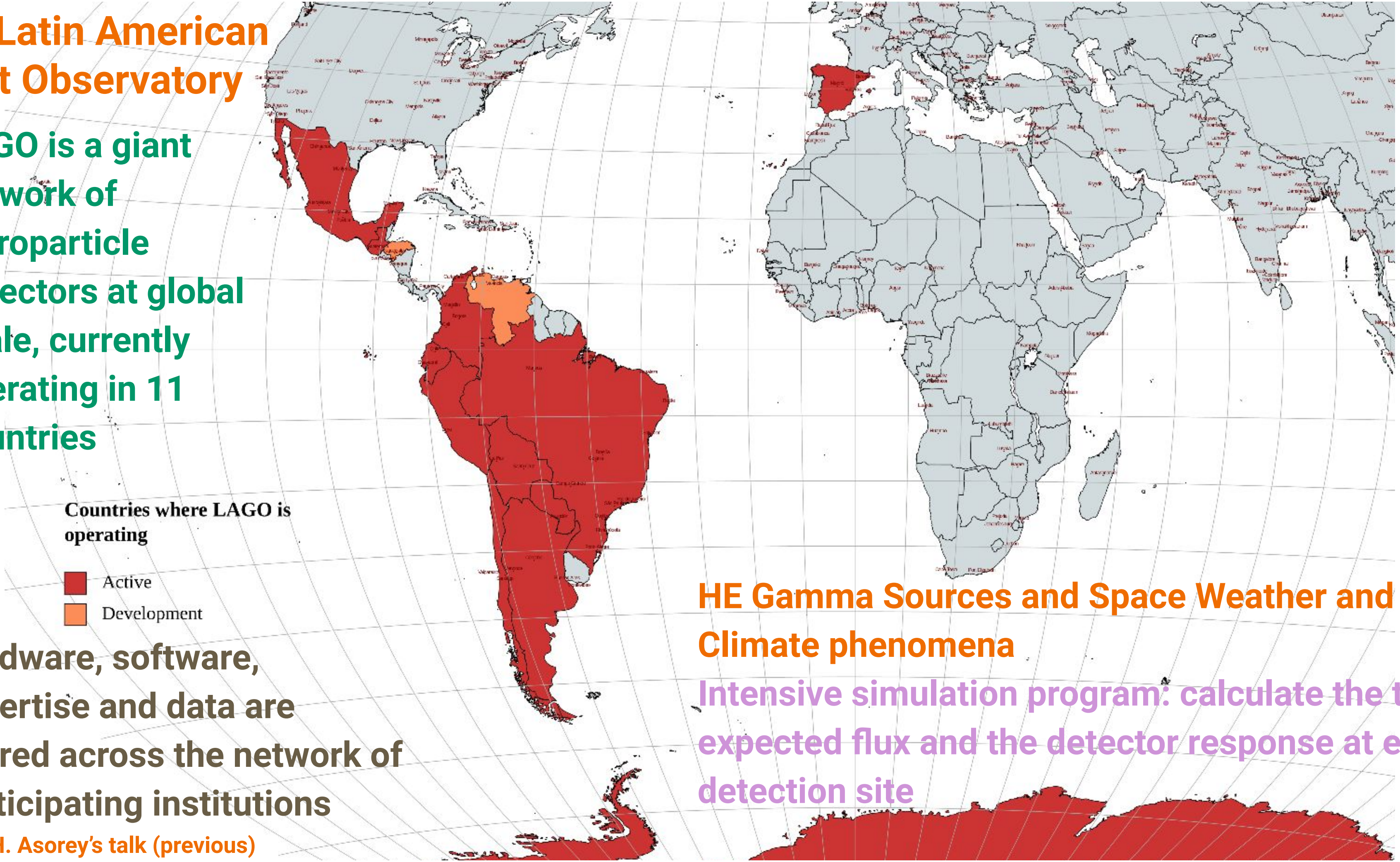

Hardware, software, expertise and data are shared across the network of participating institutions

See H. Asorey's talk (previous)

HE Gamma Sources and Space Weather and Climate phenomena

Intensive simulation program: calculate the total expected flux and the detector response at each detection site

Extensive Air Showers (EAS): each cosmic ray interacts with the atmosphere producing a cascade of up to >10^{10} secondary particles

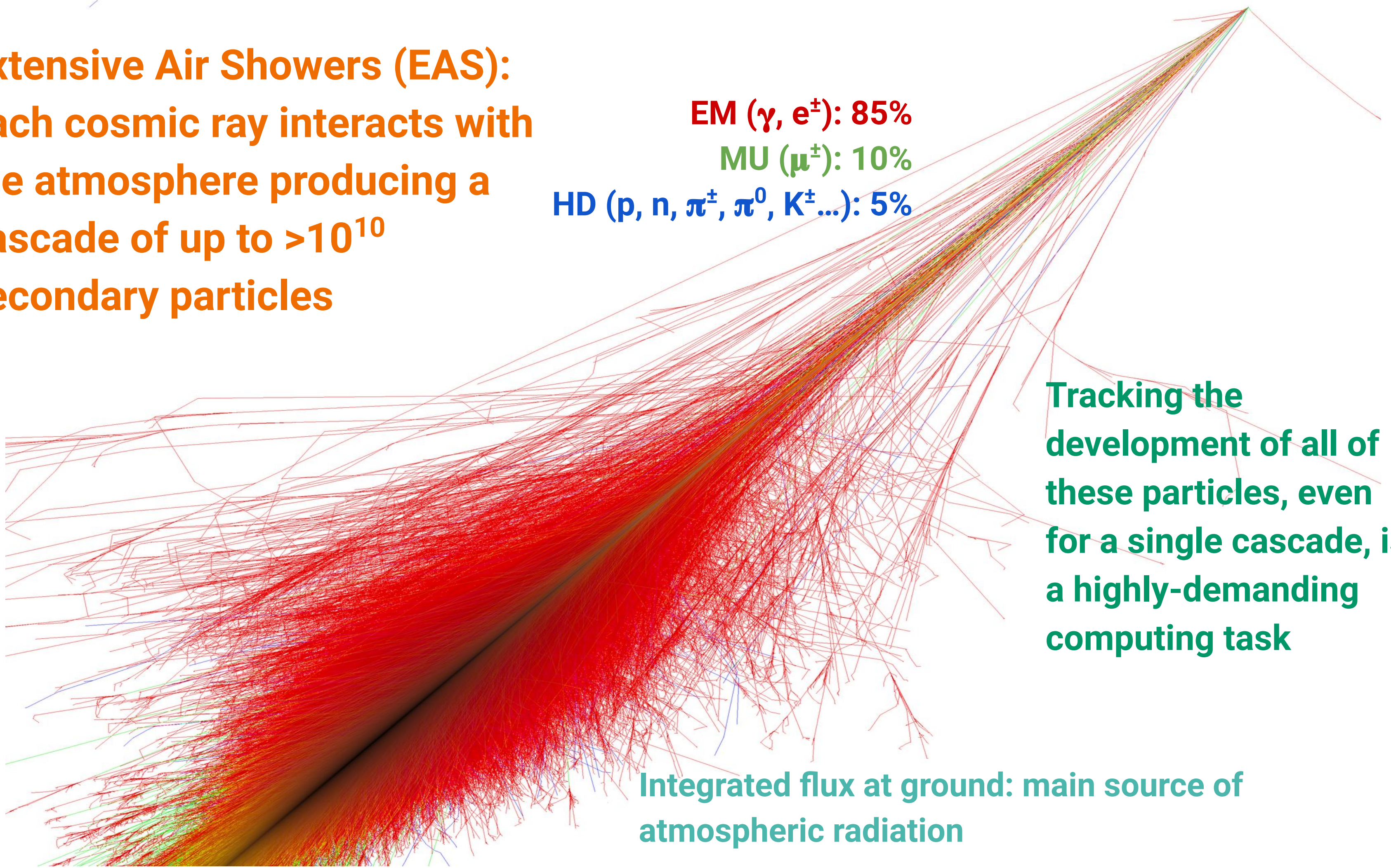

Tracking the development of all of these particles, even for a single cascade, is a highly-demanding computing task

Integrated flux at ground: main source of atmospheric radiation

From primary flux to applications

GCR Flux → Heliosphere → **Modulated Flux** → Magnetosphere → **Primaries** → Atmosphere → **Secondaries** → Detector → **Signals or Doses**

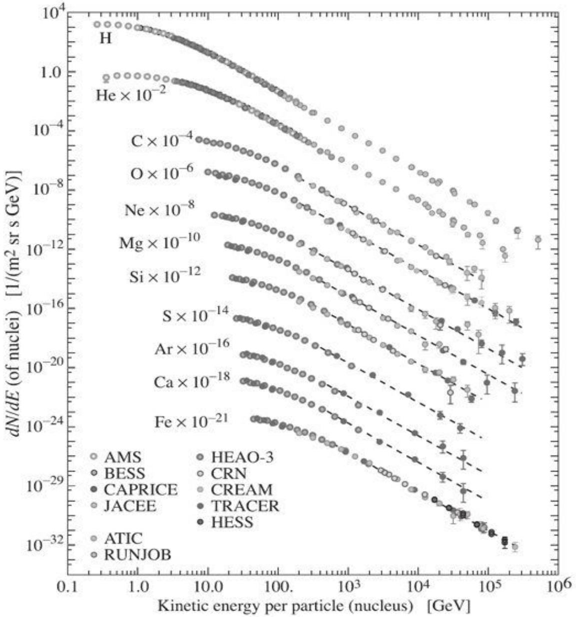

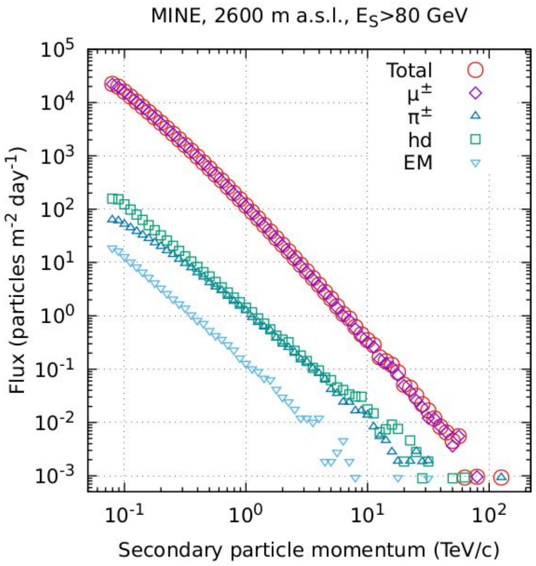

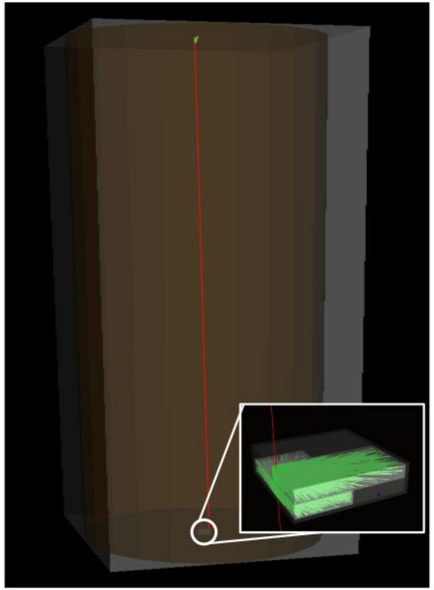

ARTI + CORSIKA **ARTI** **ARTI + Geant4**

C. Sarmiento Cano et al., EPJ C in press, 2022, arXiv:2010.14591

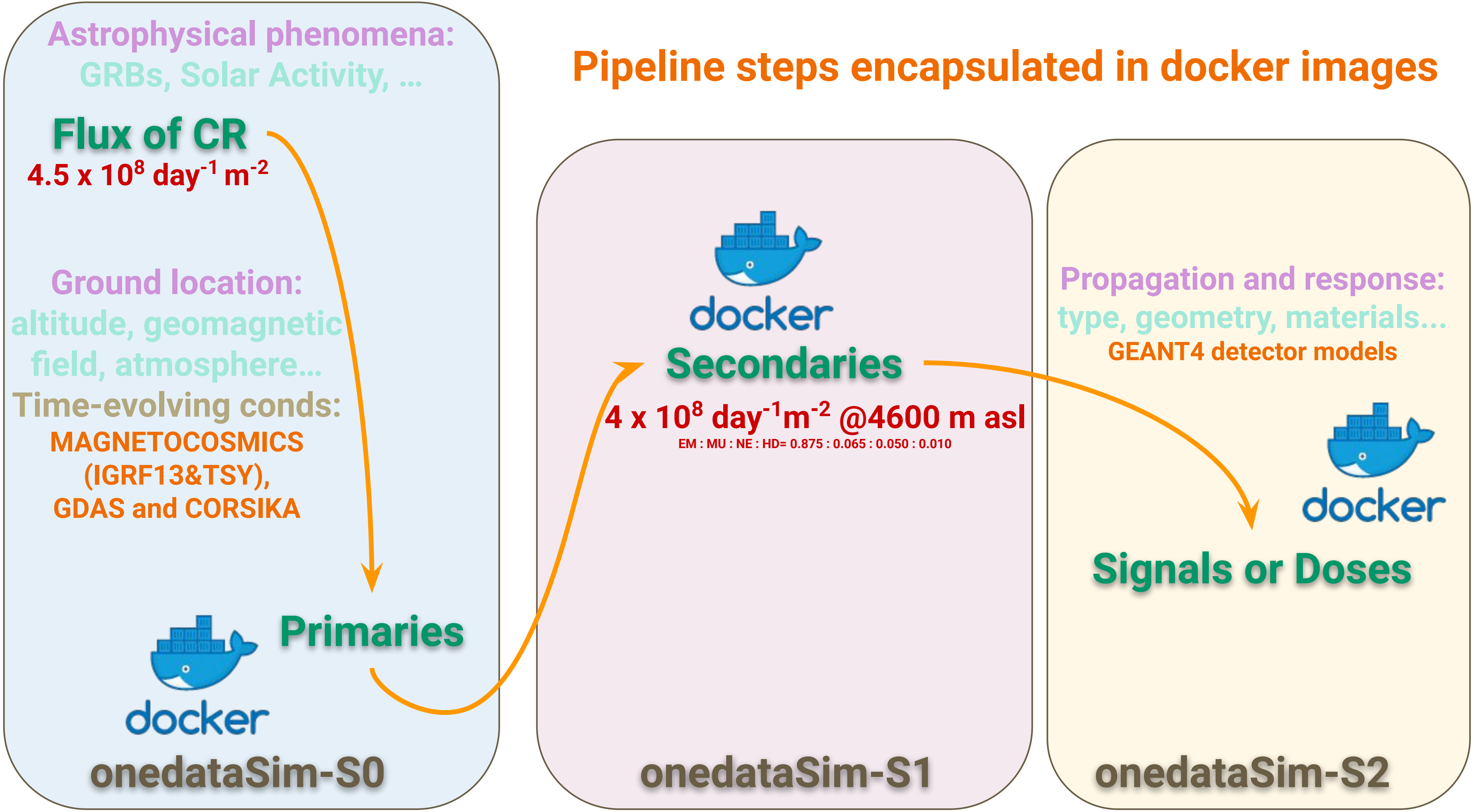

Pipeline steps encapsulated in docker images
Astrophysical phenomena:
GRBs, Solar Activity, ...
Flux of CR
4.5 x 10^8 day^-1 m^-2
Ground location:
altitude, geomagnetic field, atmosphere...
Time-evolving conds:
MAGNETOCOSMICS (IGRF13&TSY), GDAS and CORSIKA
docker
Primaries
onedataSim-S0
docker
Secondaries
4 x 10^8 day^-1m^-2 @4600 m asl
EM : MU : NE : HD= 0.875 : 0.065 : 0.050 : 0.010
onedataSim-S1
Propagation and response:
type, geometry, materials...
GEANT4 detector models
docker
Signals or Doses
onedataSim-S2

New detectors, integrated dose and better shieldings for HPC computer facilities

Detailed flux of of secondary particles at any location **around the World.**

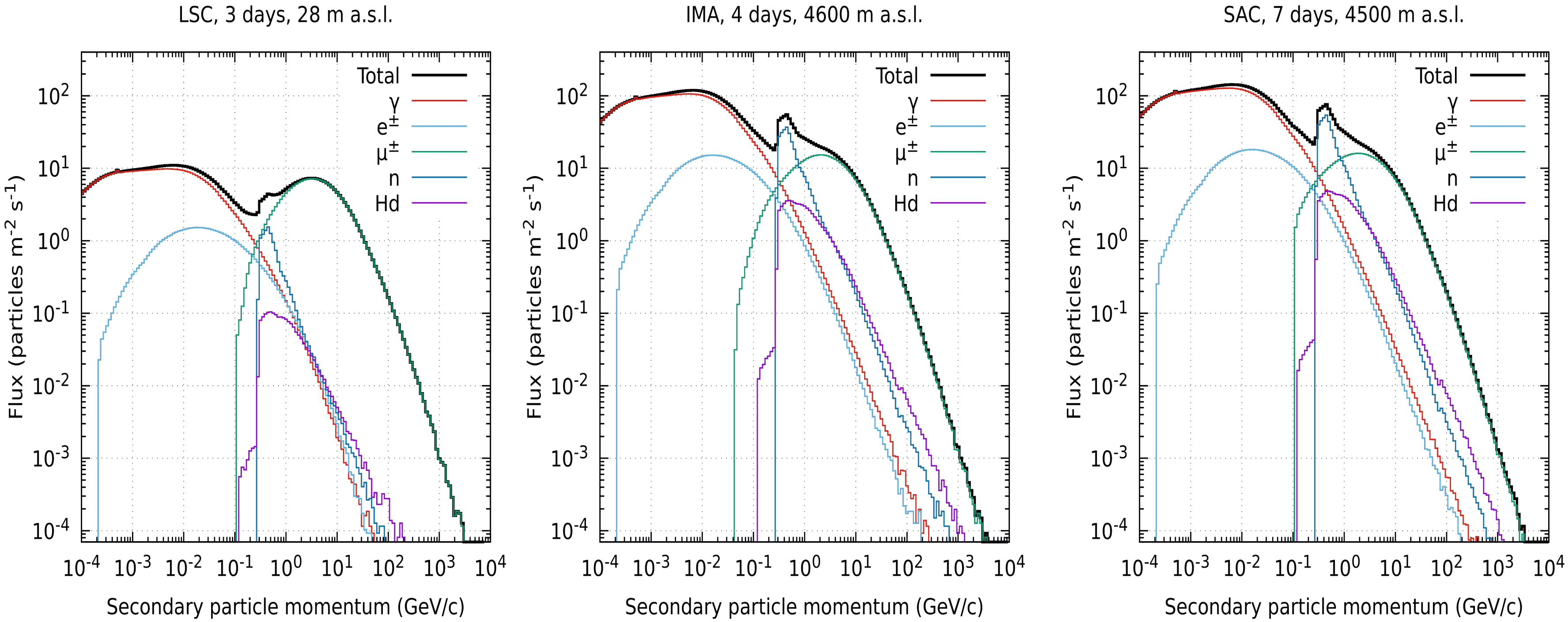

Normalised secondary particle flux at different sites in LA

AJ Rubio-Montero et al., (ICRC 2021), DOI:10.22323/1.395.0261

Atmospheric reaction produces background radiation

At 12-14 km, sea level flux times 10^2-10^3

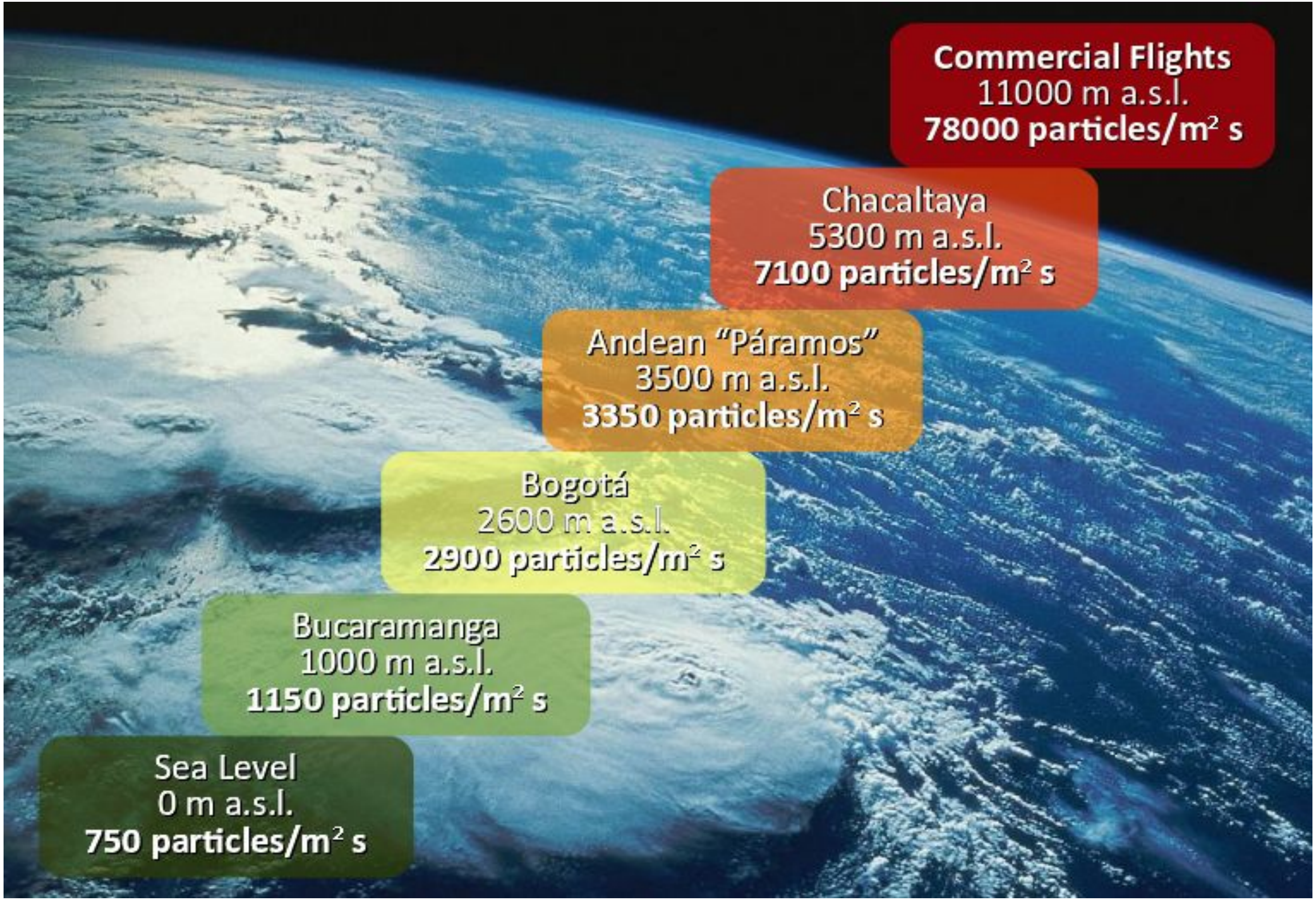

ACORDE: Application COde for the Radiation Dose Estimation

1. Segmentation of real flight paths from public databases

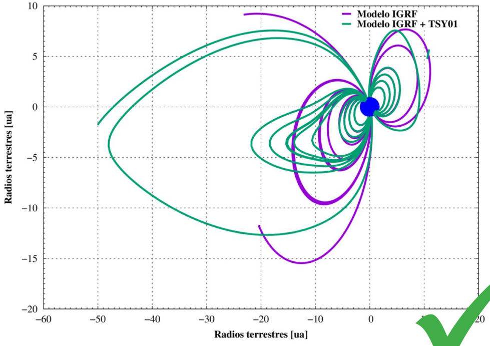

2. On route real-time geomagnetic field condition (IGRF13+TSY01)

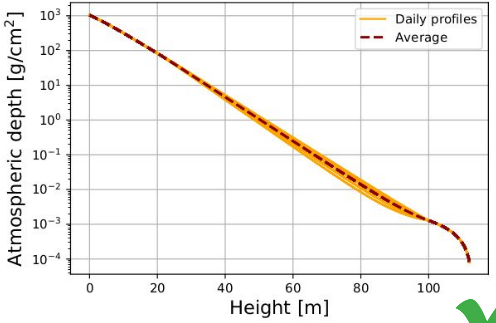

3. On route GDAS atmospheric profiles

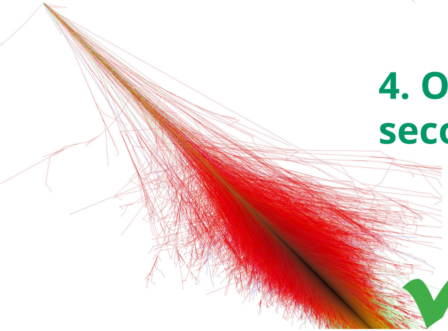

4. On route integrated secondary particles flux

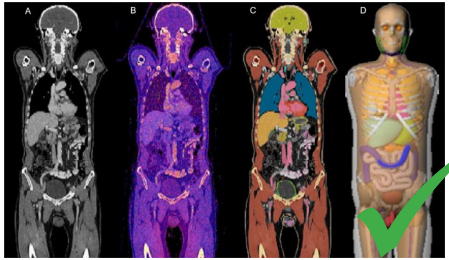

5. Effective dose calculation from Geant4 plane model and human phantoms

H. Asorey, M. Suárez-Durán and R. Mayo-García, Space Weather, in preparation, 2022

ACORDE example: comparative altitude effect

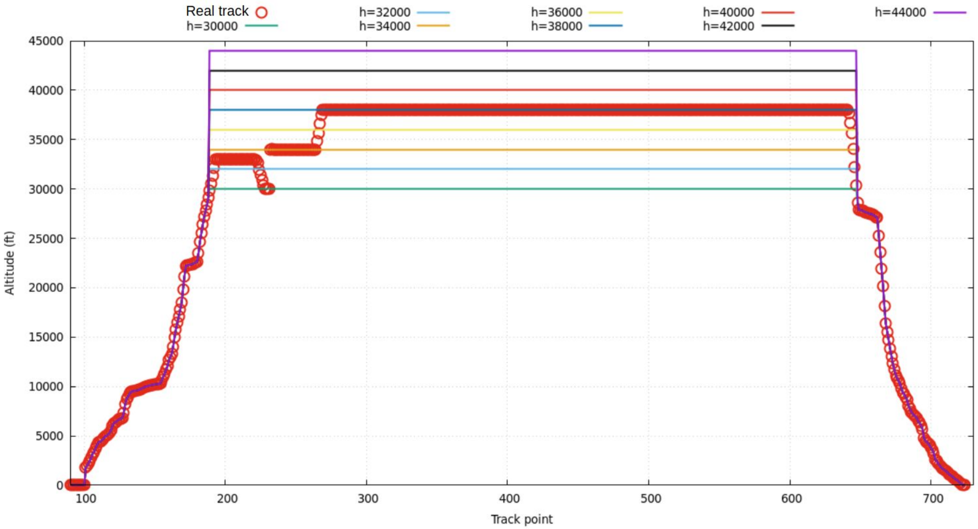

Same flight under the same conditions but only varying altitude

calculated dose reference: 100 μSv
> 2.5x at 44,000 ft (resp 30,000 ft)

Altitude (feet)	Acorde	CARI 7A
30.000	1,00	1,00
32.000	1,24	1,20
34.000	1,49	1,42
36.000	1,77	1,65
38.000	2,05	1,89
40.000	2,38	2,14
42.000	2,69	2,38
44.000	3,00	2,64
Measured track (relative to 30,000 ft)	***1,74***	***1,62***

H. Asorey, M. Suárez-Durán and R. Mayo-García, Space Weather, in preparation, 2022

ACORDE: Application COde for the Radiation Dose Estimation

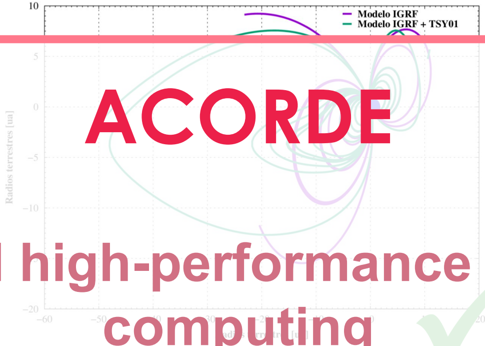

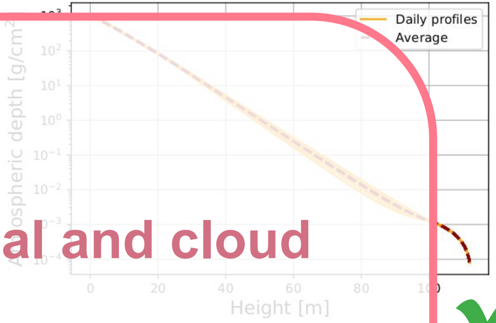

ACORDE

→ Self-managed high-performance local and cloud computing

→ Cloud based dosimetry calculations in Geant4 (with applications in radiotherapy)

→ Software as a Service (SaaS) capable implementation

1. Segmentation of real flight paths from public databases

2. On route real-time geomagnetic field condition (IGRF13+TSY01)

3. On route GDAS atmospheric profiles

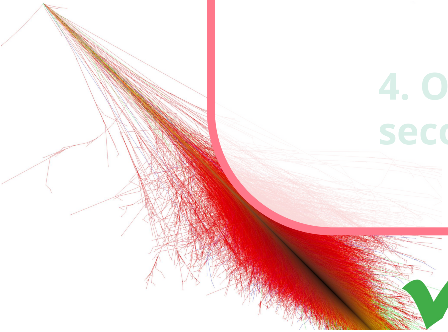

4. On route integrated secondary particles flux

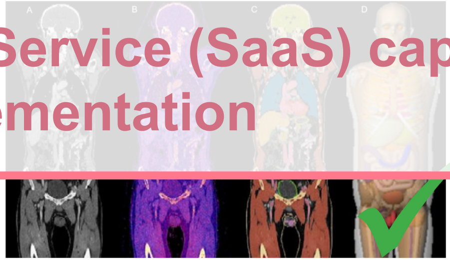

5. Effective dose calculation from Geant4 plane model and human phantoms

H. Asorey, M. Suárez-Durán and R. Mayo-García, Space Weather, in preparation, 2022

Muography: muon radiography of large structures

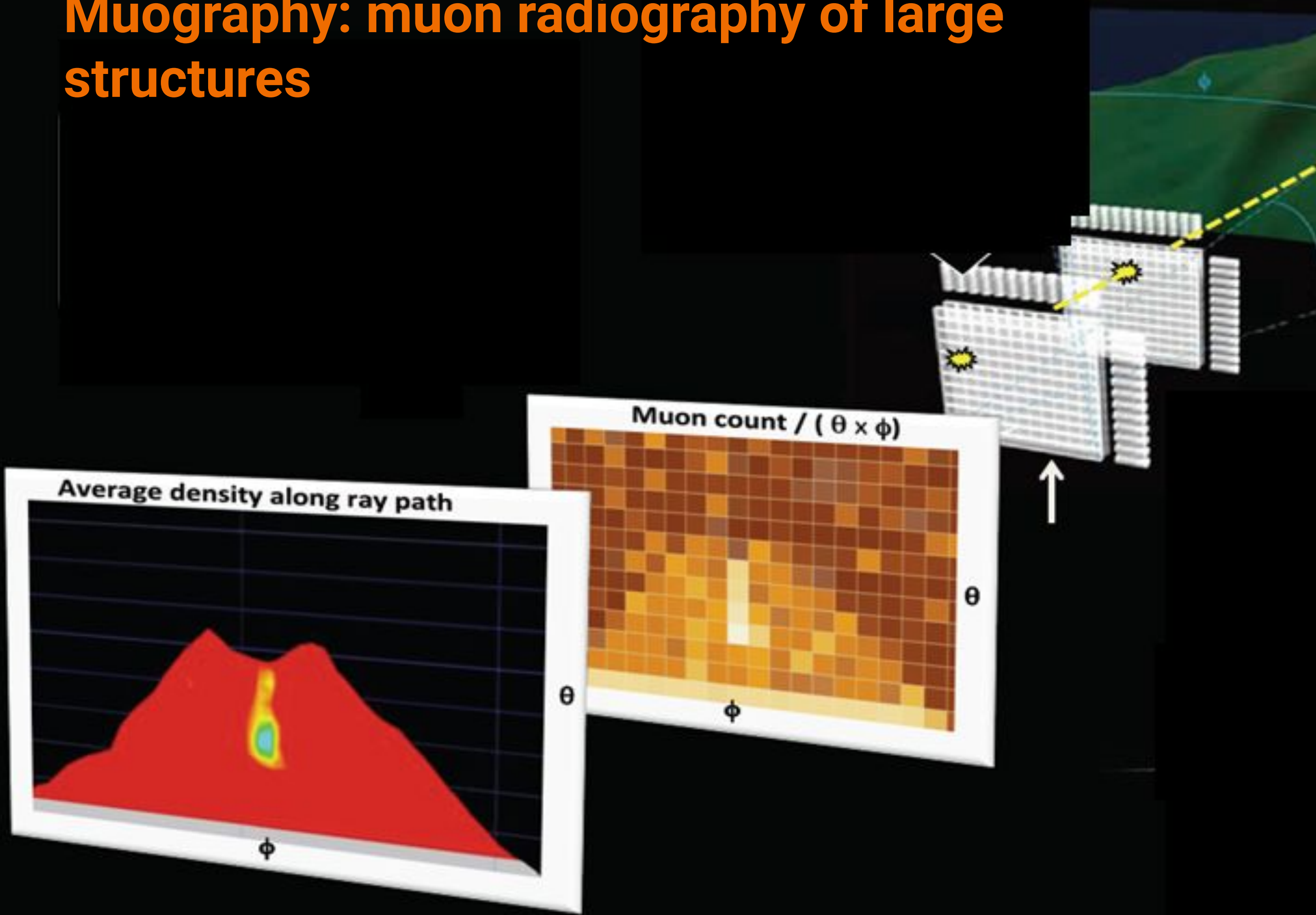

Muography, how to

- Start with an object with an unknown density profile
  - … measure the directional muon flux through this object
  - … and compare with the muon reference flux
  - → **you get the directional opacity of this object [g/cm²]**
- Additionally…
  - … obtain the external geometry of the object
  - → **and calculate the directional interaction distance [cm]**
- Finally, from…
  - directional opacity
  - directional interaction distances
- → **get internal density profile along muon propagation direction**

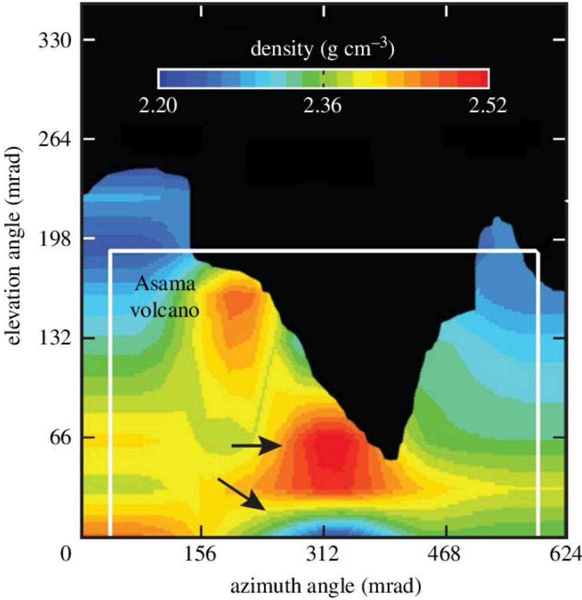

$$\varrho(L) \equiv \int_L \rho(\xi)\,\mathrm{d}\xi,$$

Modulus, our modular design

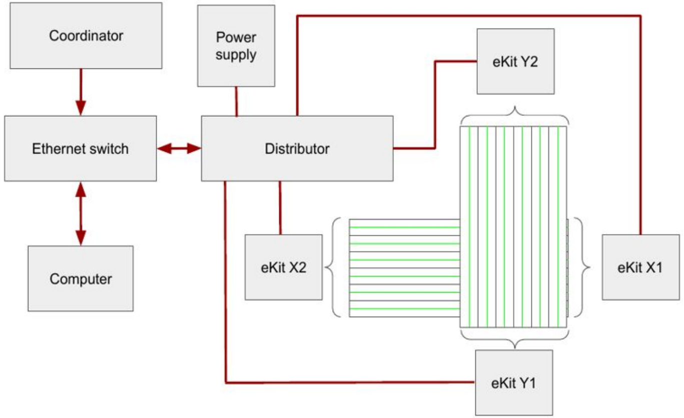

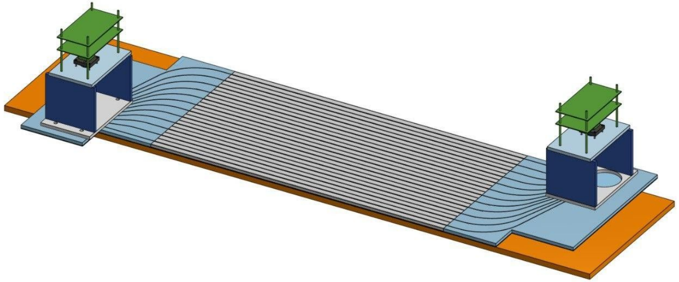

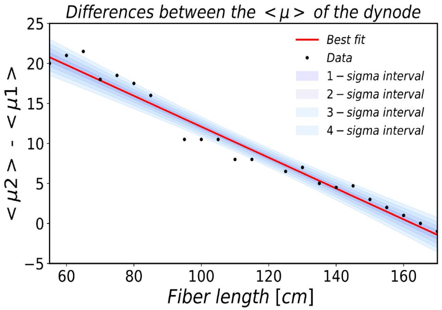

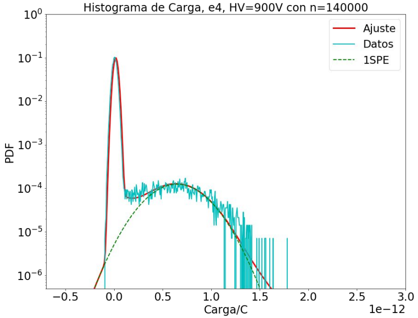

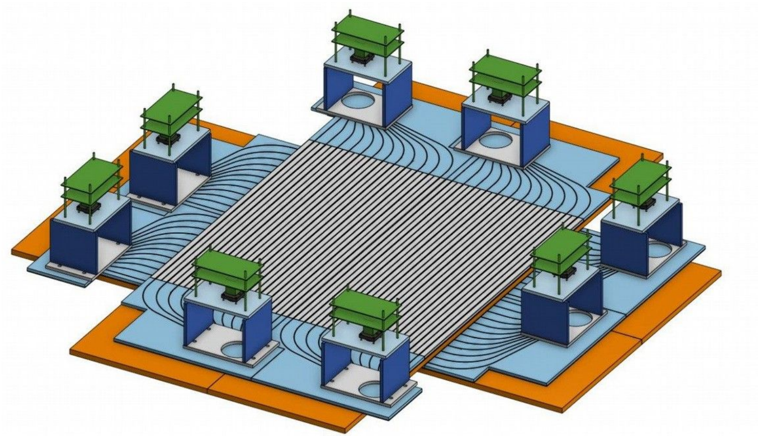

$$S_{real}(x) = S_{ideal}(x) \otimes N(x)$$

$$S_{ideal}(x) = \sum_{n=0}^{\infty} \frac{u^n \cdot e^{-u}}{n!} \cdot \frac{1}{\sigma\sqrt{2\pi}} \cdot e^{-\frac{(x-n\cdot q)^2}{2n\sigma^2}}$$

Calderón-Ardila et al, JAIS 2022.300, 2022

First functional prototype

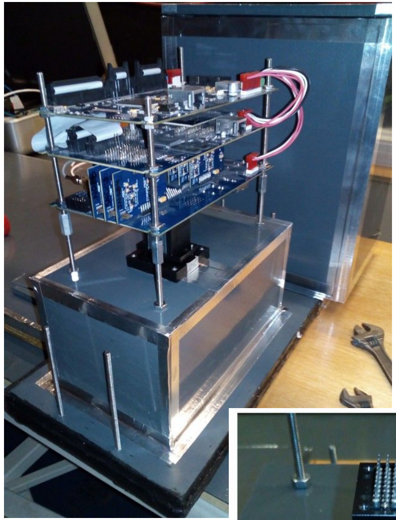

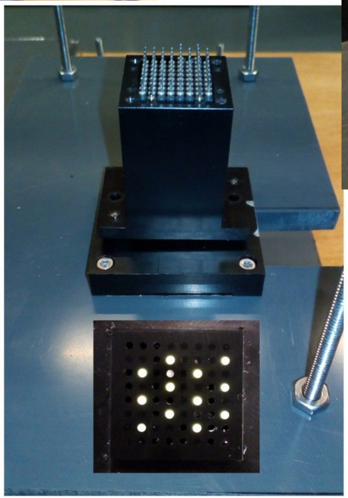

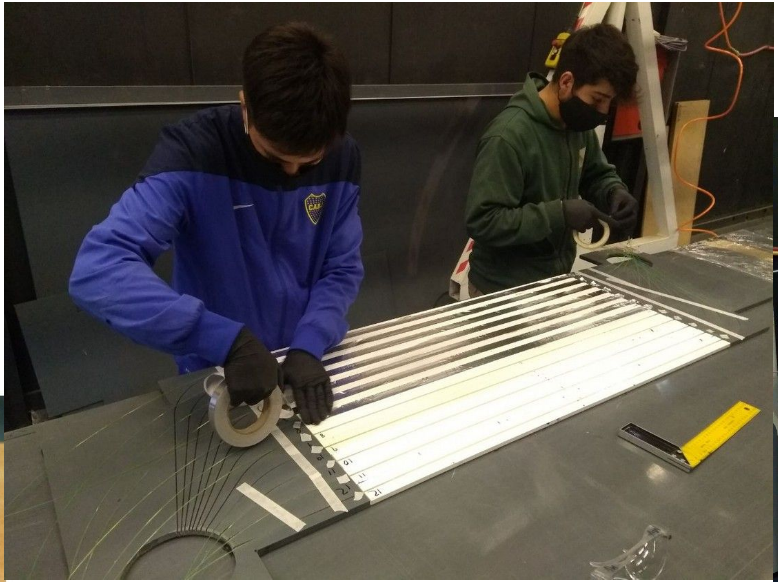

Technology transference from astroparticle detection to muography

Modular assembly, calibration, testing and coincidence detection

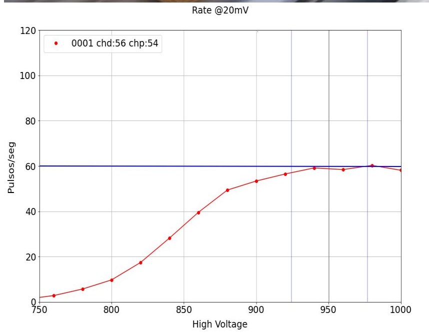

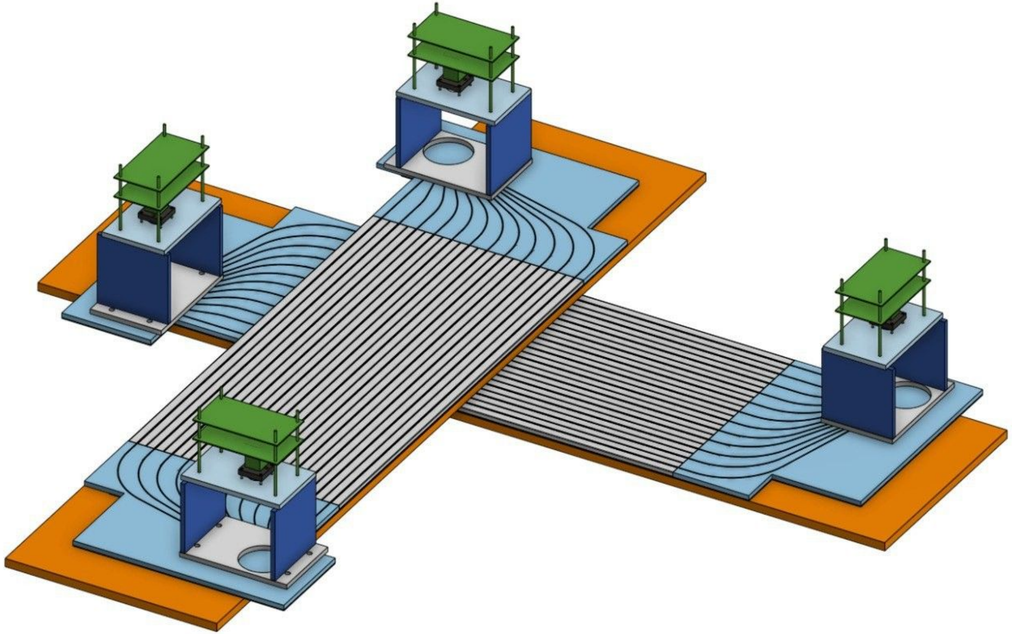

Single or double-head configurable signal acquisition electronics, depending on possible targets characteristics

Mining prospecting applications in Argentina

Detector deployment at selected site planned for 2022

Detector site is selected at 330 m depth (~900 mwe depth)

New detector geometry optimized for underground measurement

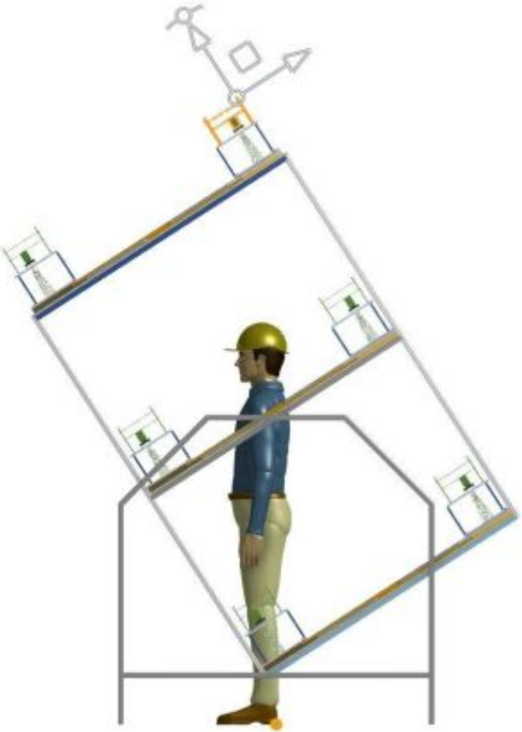

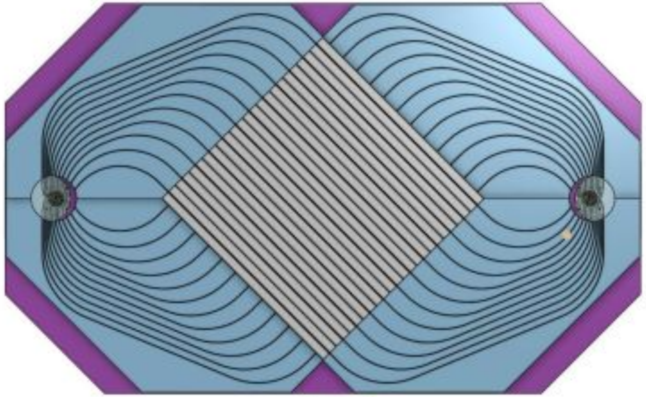

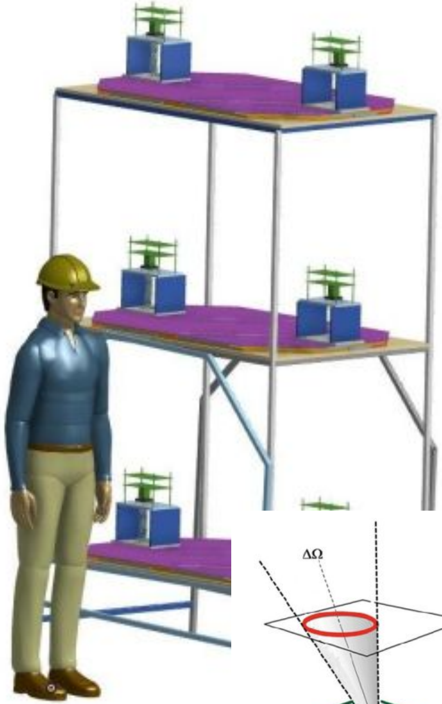

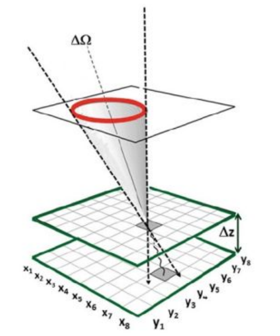

Calderón-Ardila et al, JAIS 2022.300, 2022

OneDataSim-S2: “Meiga” workflow

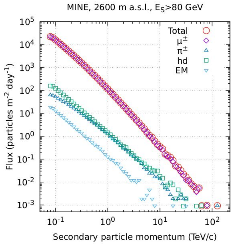

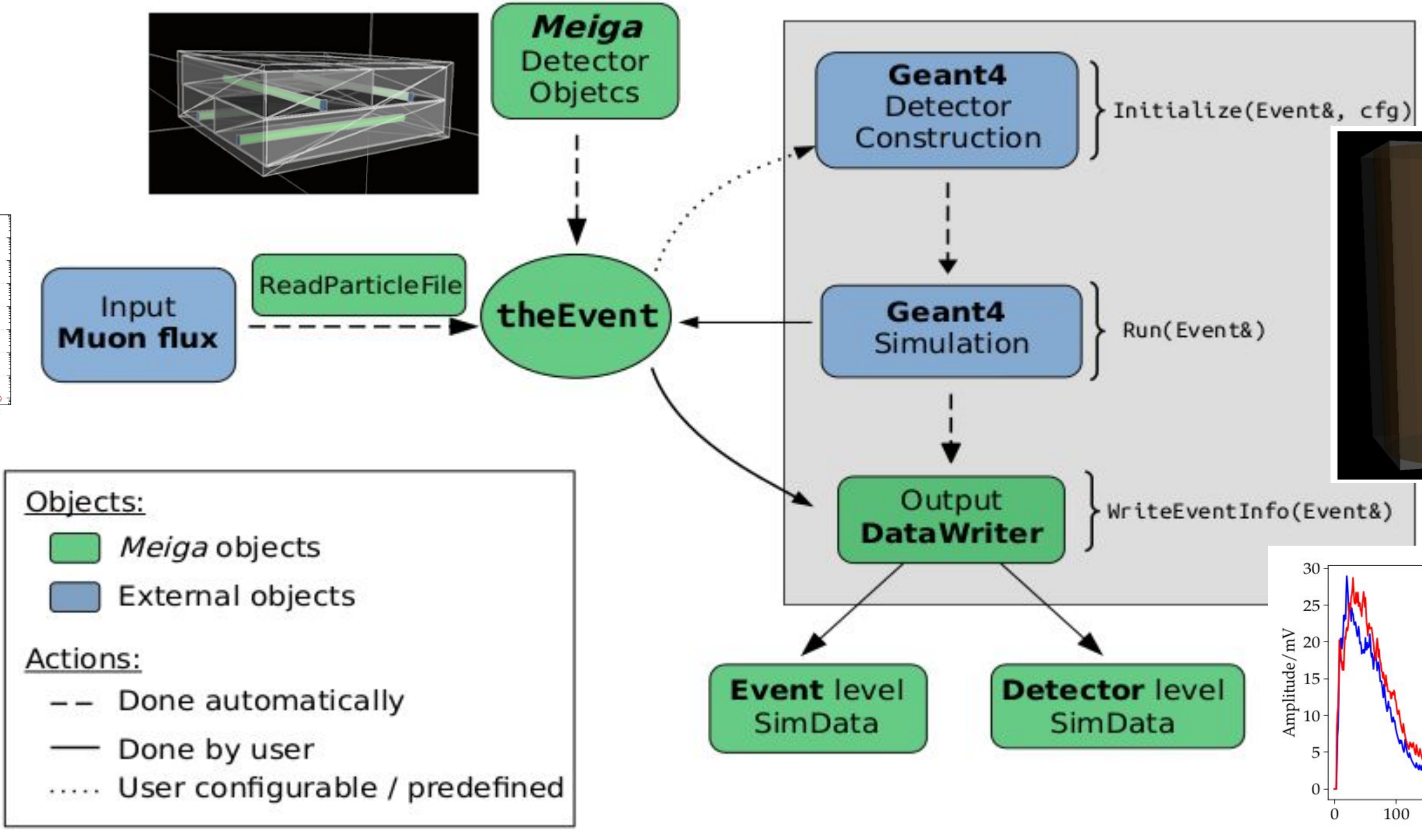

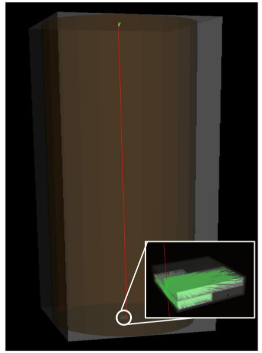

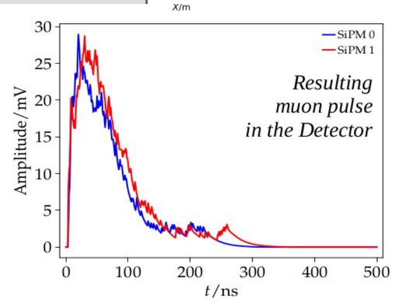

A. Taboada et al., J. Adv. Inst. Sci. 266, 2022

High-energy flux propagation through 500m of rock impinging on an underground detector

OneDataSim@cloud

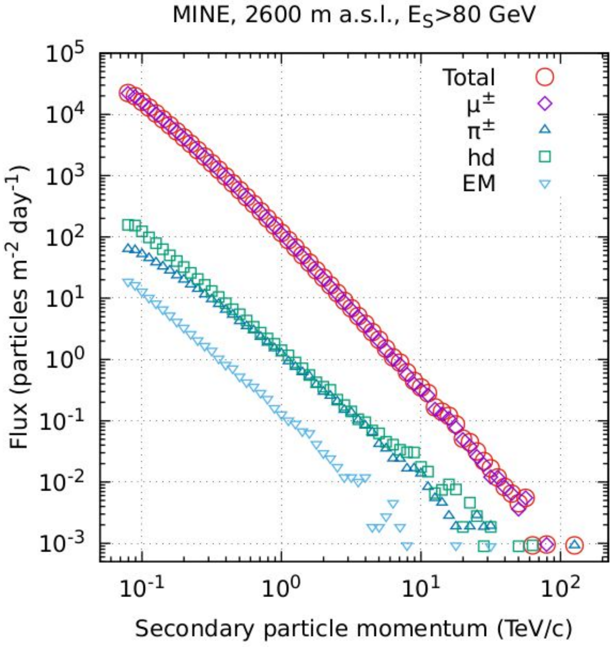

MEIGA@hpc

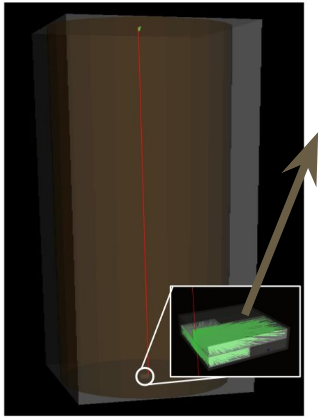

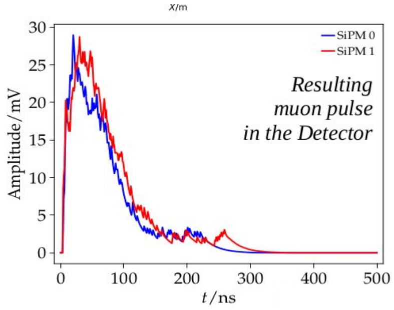

Expected detector response

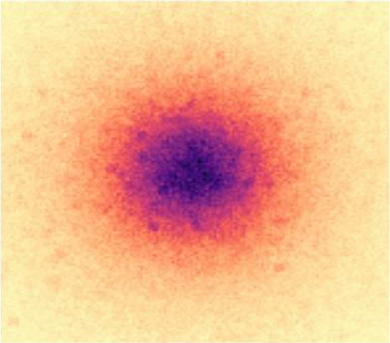

Example: change in density profile

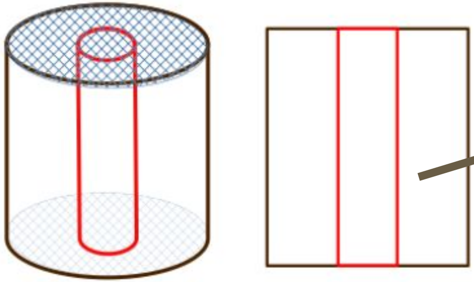

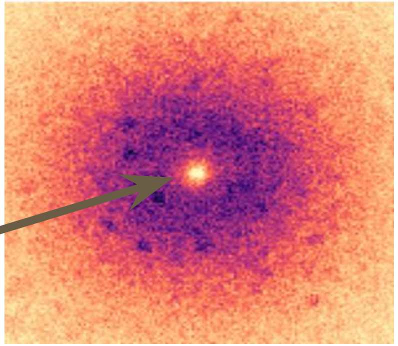

A. Taboada et al, JAIS 2022.266, 2022

The ANDES Underground Lab at the Agua Negra tunnel

Bi-national tunnel (Argentina and Chile)

Two separated tunnels of 12m diameter

14 km underground

1700m (4600 mwe) of rock coverage

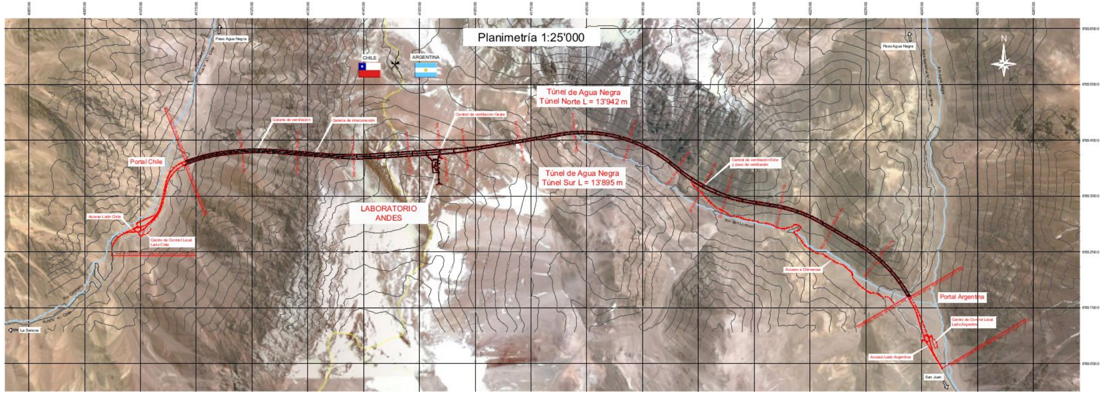

The ANDES Underground Lab at the Agua Negra tunnel

Bi-national tunnel (Argentina and Chile)

er

The ANDES Underground Lab - Detailed engineering (2019)

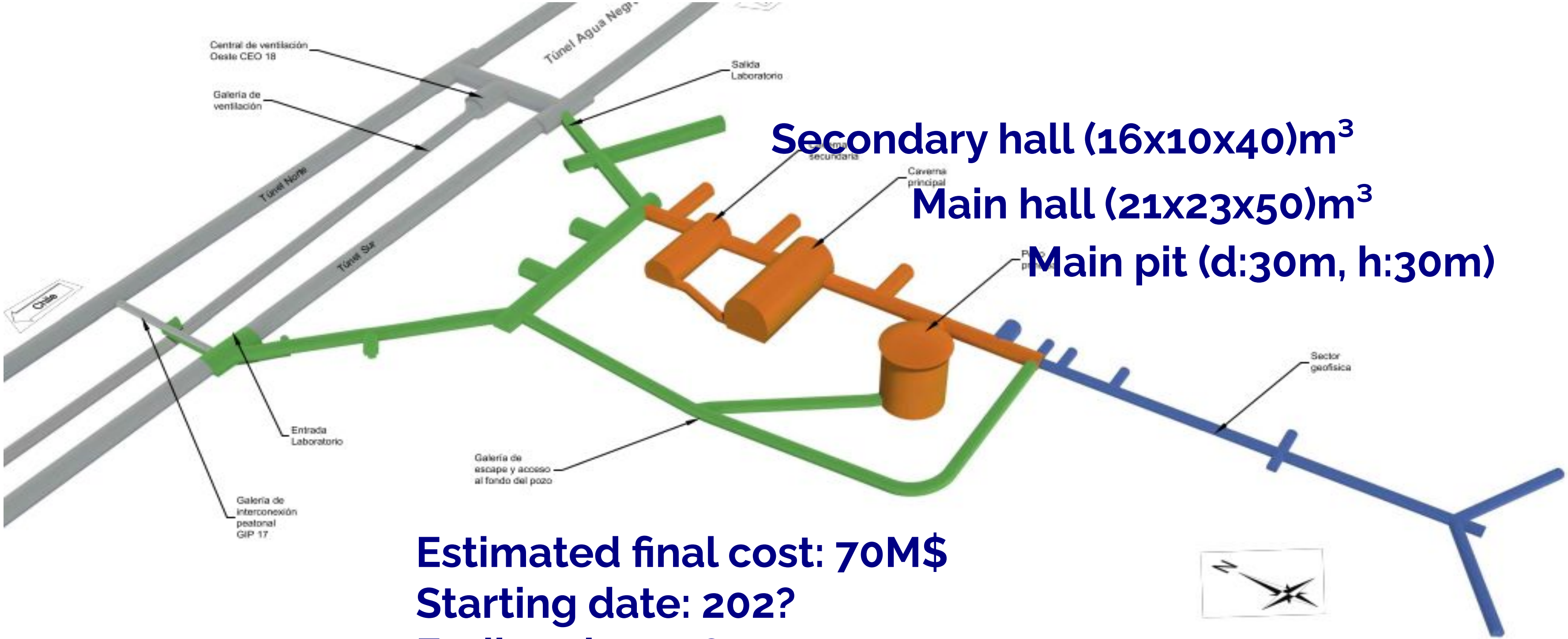

Secondary hall (16x10x40)m³

Main hall (21x23x50)m³

Main pit (d:30m, h:30m)

Estimated final cost: 70M$
Starting date: 202?
Ending date: +8

M. Gómez-Berisso, Hernán Asorey, X. Bertou, CNEA internal technical report, (2019)

Muography and Underground LABs

One-year simulated flux of secondary particles at ground level (~1.5 kCPU·h/site)

MINE, 900 m.w.e., p_{CUT}=80 GeV/c

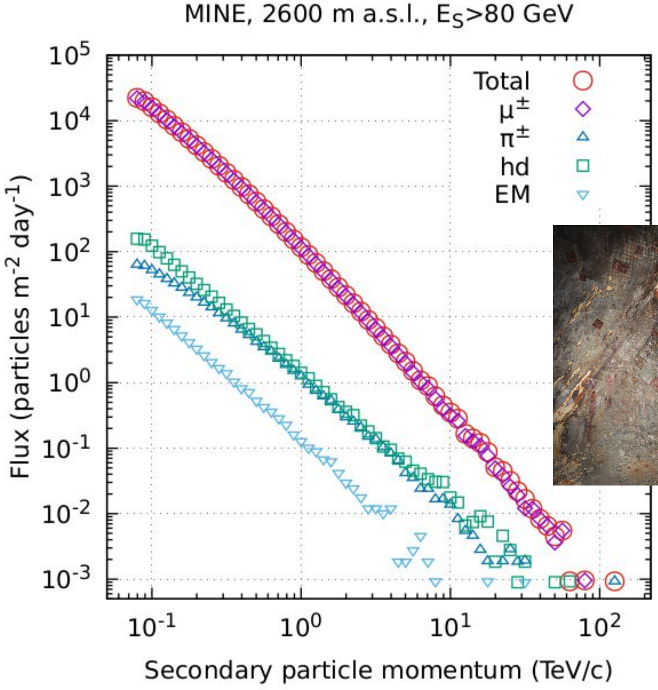

ANDES, 4600 m.w.e., p_{CUT}=800 GeV/c

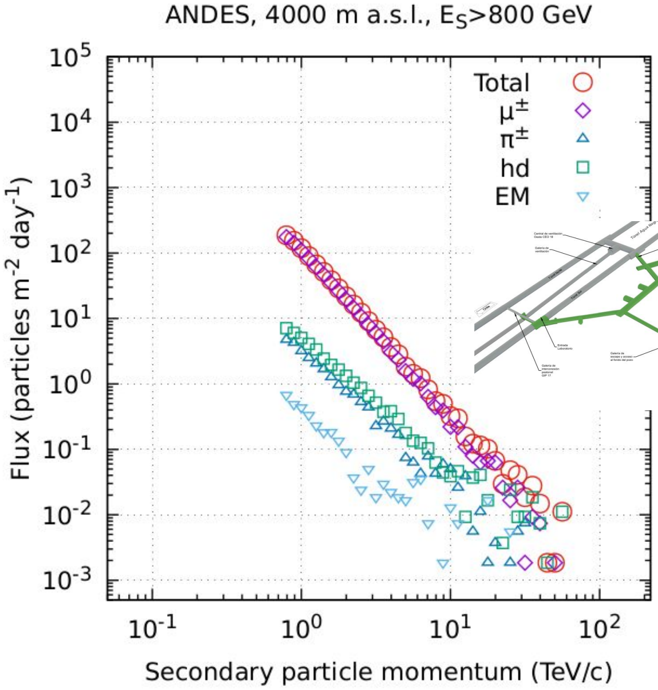

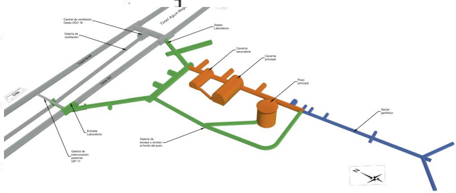

Normalised high-momentum (p_s>p_{CUT}) secondary particle at different sites around the World

R. Calderón-Ardila et al., J. Adv. Inst. Sci. 300, 2022; A.J. Rubio-Montero et al., (ICRC 2021), DOI:10.22323/1.395.0261

ANDES: under 1700m of rock neutrino physics and DM searches

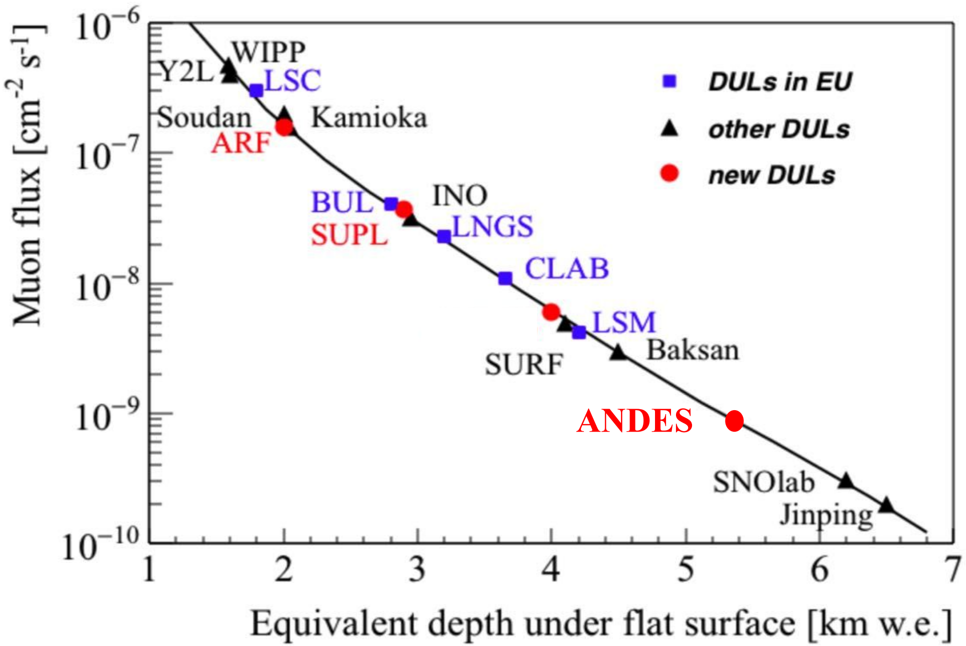

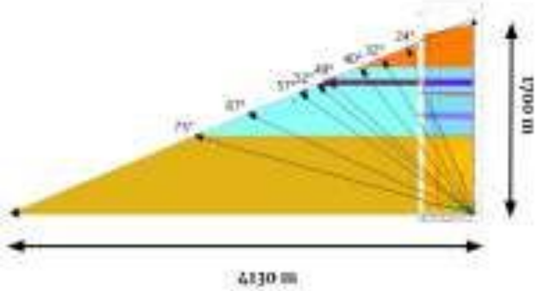

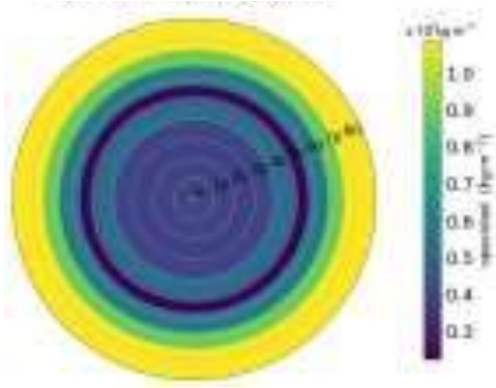

$\Phi_\mu < 5 \times 10^{-9}$ cm^{-2} s^{-1}

Carmina Pérez-Bertoli, "Best underground thesis in Physics 2020 Award"; C. Pérez-Bertoli, C. Sarmiento-Cano and H. Asorey, AFA annals 32(4) 106, 2022

The age of exascale computing is here

23 new exascale supercomputing centres are being built around the World
High- and low-energy neutrons are one of the main sources of Silent (undetected) Errors

H. Asorey and R. Mayo-García, J. Supercomputing, submitted, 2022

Seasonal variations and real atmospheric effects on HE neutrons

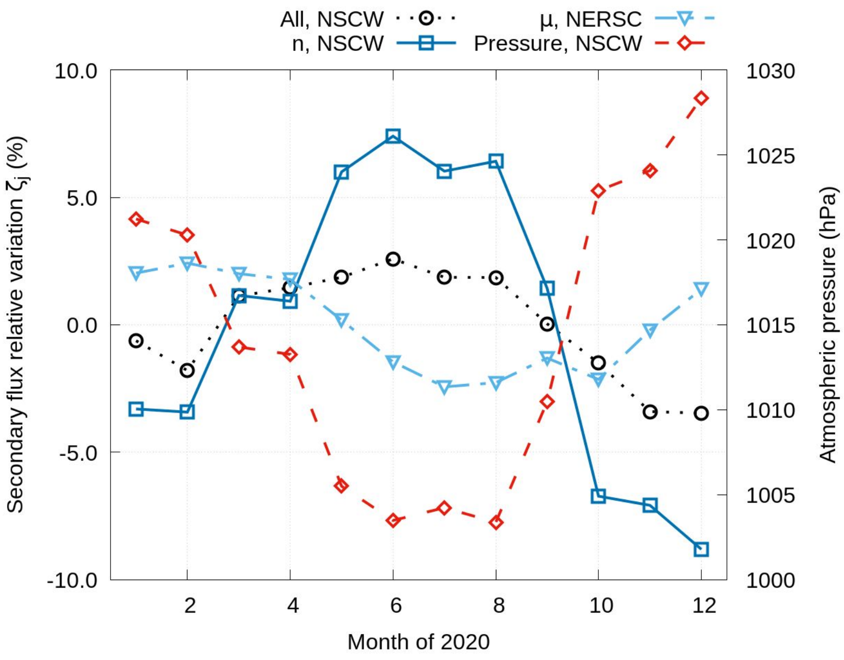

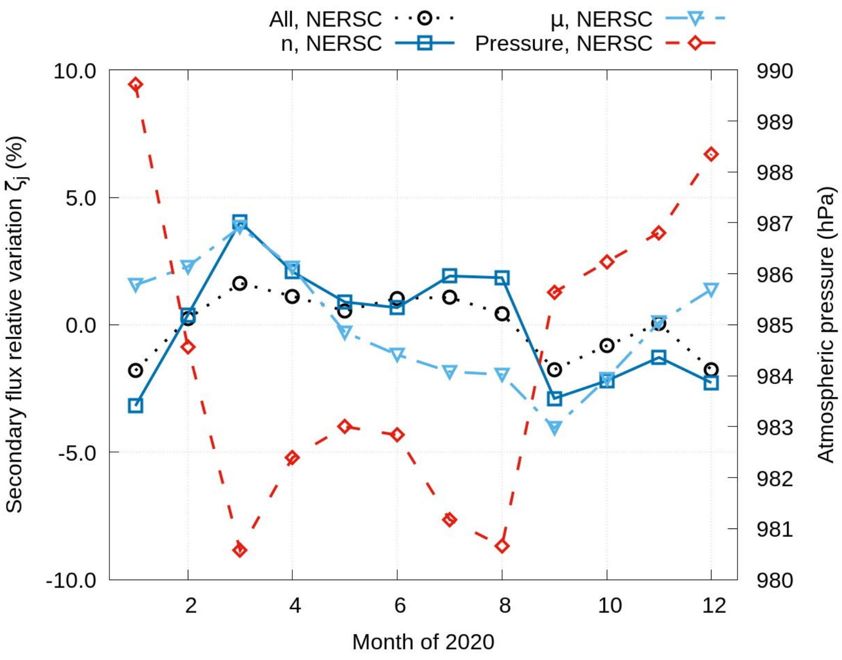

For each centre, real GDAS atmospheric profiles and geomagnetic conditions were extracted and relative variations were computed

H. Asorey and R. Mayo-García, J. Supercomputing, submitted, 2022

Barometric coefficients β and Failure in Time rates at each site

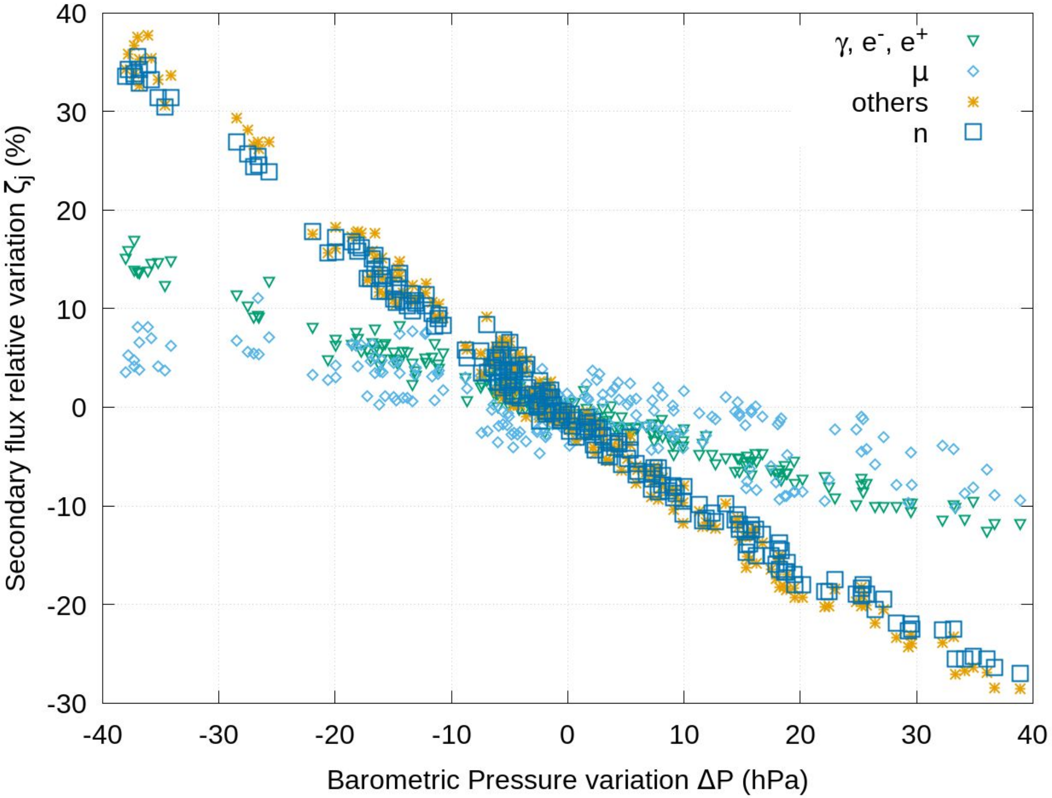

- Atmospheric impact depends on secondary particle type
- neutrons are the most affected
- Barometric coefficients β were calculated for each site
- From β and averaged values at each site is it possible to calculate the failure-in-time rates:

$$\mathrm{FIT}_{\mathrm{err}}(t) = 10^5\ \sigma_{\mathrm{err}}\ \overline{\Xi_i}\left[1 + \beta_i\left(P(t) - \overline{P}\right)\right]$$

- And then, the expected MTBF (mean time between failures):

$$\mathrm{MTBF}_{\mathrm{err}}(t) = \frac{10^9}{\mathrm{FIT}_{\mathrm{err}}(t)}\mathrm{hours}$$

During a thunderstorm, ΔP~-5 hPa, and so, at, e.g., Titan, silent errors MTBF ~1 day

H. Asorey and R. Mayo-García, J. Supercomputing, submitted, 2022

Conclusions: ARTI+MEIGA

□ **detailed flux of secondary particles, signals or doses at any altitude around the World, under realistic atmospheric and geomagnetic conditions.**

□ **ARTI incorporate state-of-the-art astroparticle simulations techniques, and was intensively tested and verified by several astroparticle observatories. MEIGA allows the possibility to easily evaluate very different detector types and materials and geometries**

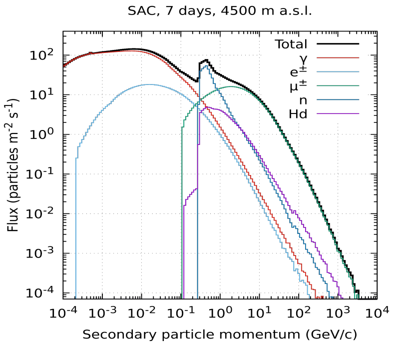

New astroparticle observatories and detectors

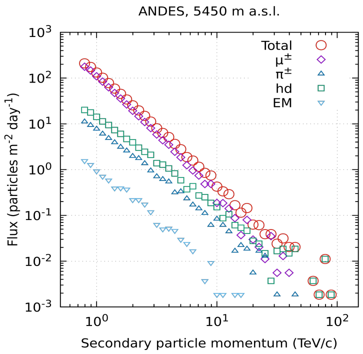

Muon flux for muography applications and underground labs

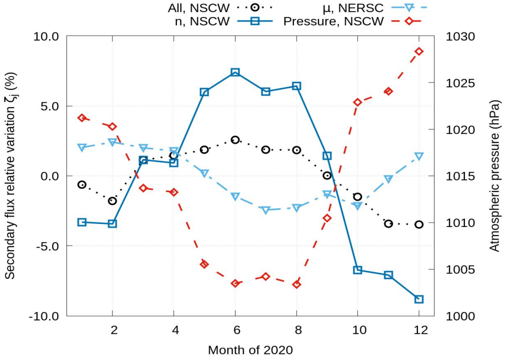

HE neutron flux and failure rates estimation at supercomputing centres

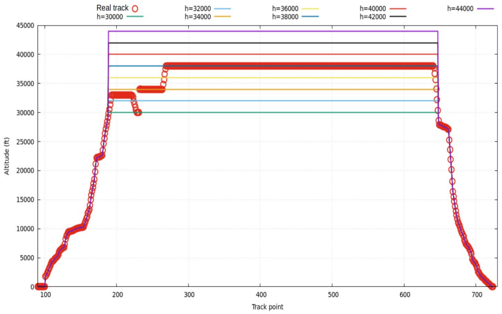

Effective dose calculation at commercial flights in realistic conditions

□ **ARTI is publicly available at the LAGO GitHub repo: github.com/lagoproject/arti**

Thank you for your attention

primary flux integration

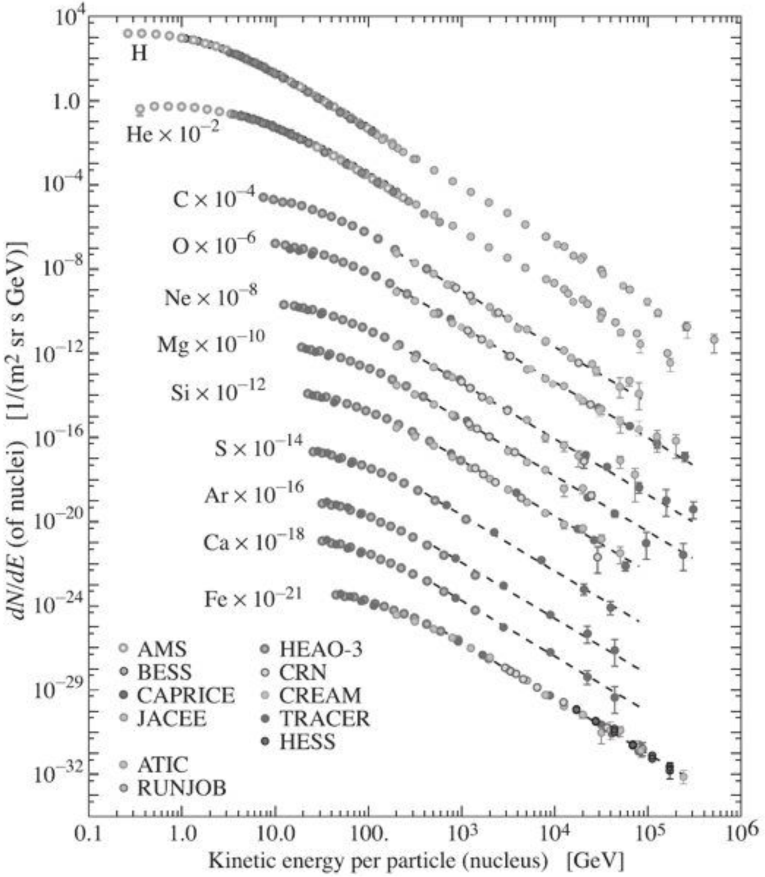

For each primary, we need to integrate its spectrum to get the expected number of primaries at the top of the atmosphere

$$N_{t,S} = \int_t \int_S \int_\Omega \int_{E_p} j_0(E_p, Z_p)^{\alpha(E_p,Z_p)}\, dt\, dS\, d\Omega\, dE$$

We integrate:

- full spectra, $1 < Z < 26$
- hemisphere, $0 \leq \theta \leq \pi/2, -\pi \leq \phi \leq \pi$
- energy range, $(R_C \times Z_p) < E/GeV < E_{\max}$

R_C is the local, time-dependent, geomagnetic rigidity cut-off
E_{max} depending on application

M. Suárez-Durán, H. Asorey and L.A. Núñez, Space Weather, (2018), DOI:10.1002/2017SW001774

time-dependent local geomagnetic effects

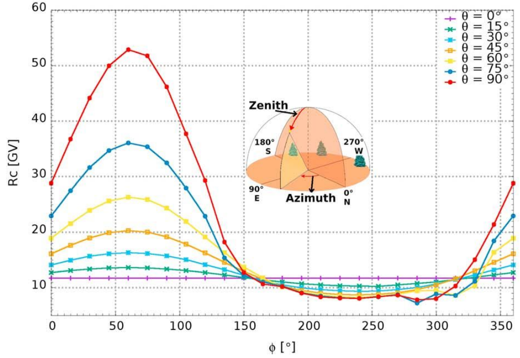

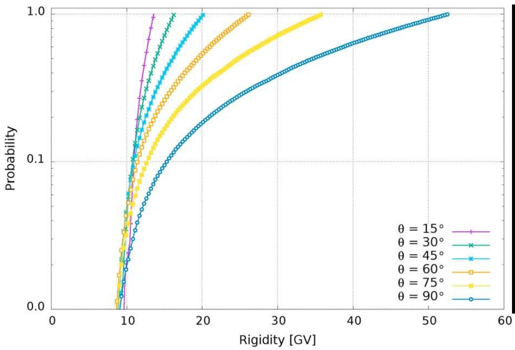

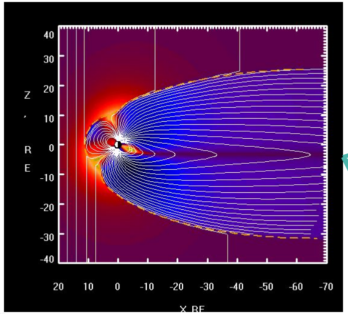

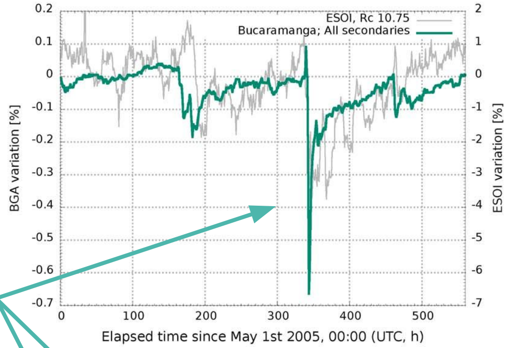

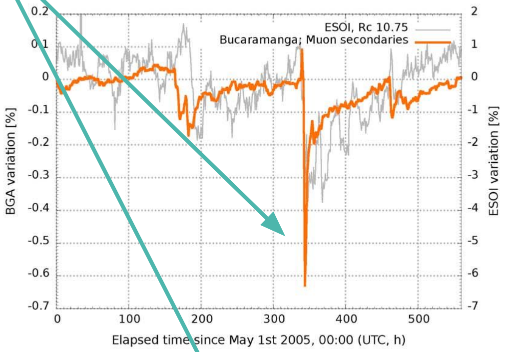

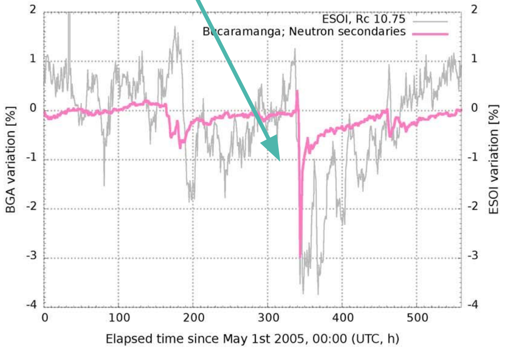

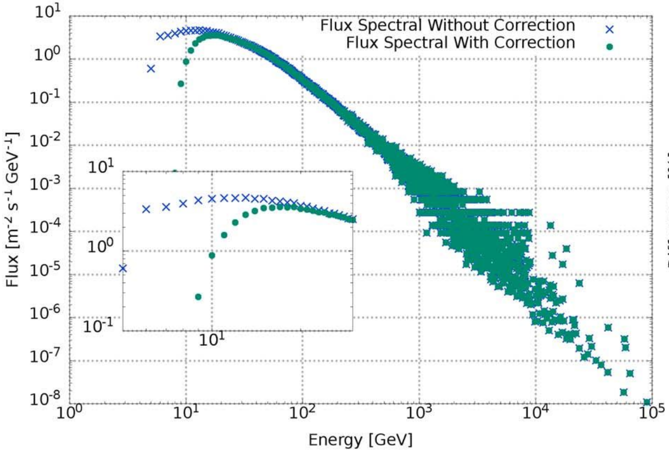

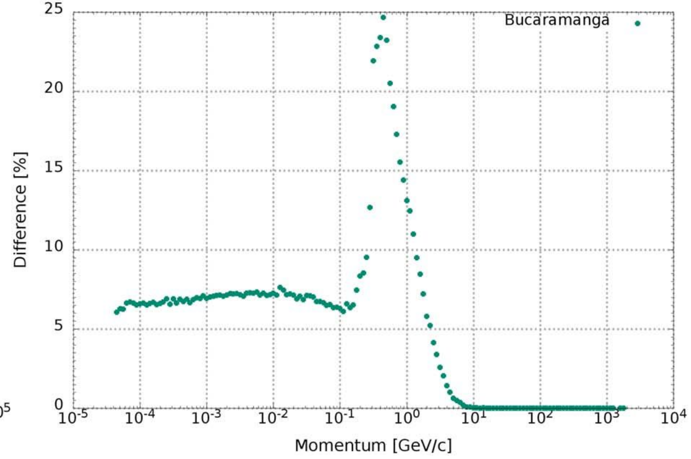

M. Suárez-Durán, H. Asorey and LA Núñez, Space Weather, (2018), [DOI:10.1002/2017SW001774](https://doi.org/10.1002/2017SW001774)

local atmospheric effects

Monthly-averaged or instantaneous local atmospheric profiles from GDAS

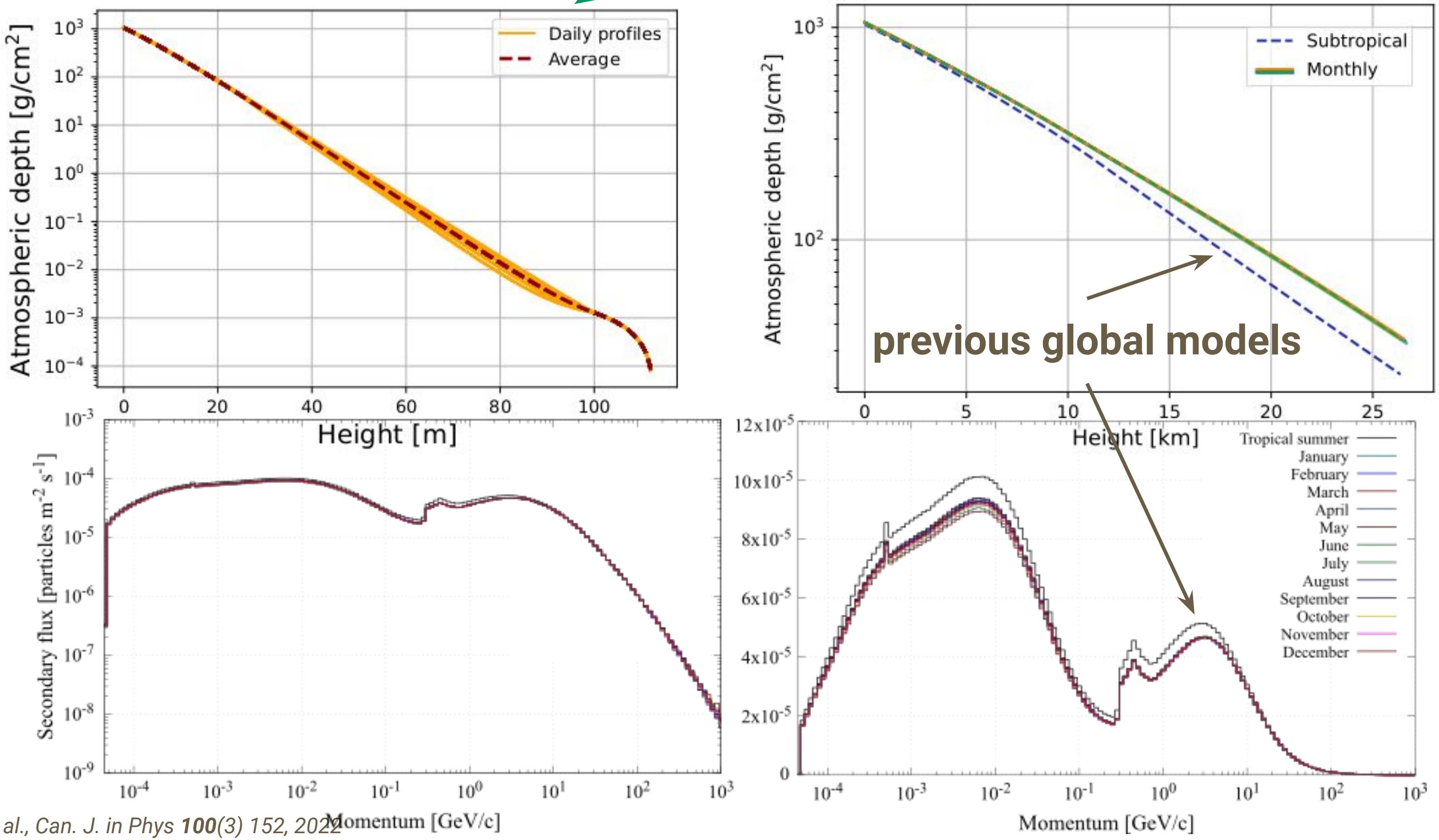

J. Grisales et al., Can. J. in Phys ***100****(3) 152, 2022*